Inorg. Chem. **2007**, *46*, 8418–8425

Cyclic Se_6 and Helical $^1_\infty[Se_x]$ as Neutral Ligands in the New Compounds $PdBr_2Se_6$ and $PdCl_2Se_8$†

Hans-Joerg Deiseroth,*,‡ Christof Reiner,‡ Marc Schlosser,‡ Xiaowen Wang,‡ Humayun Ajaz,‡ and Lorenz Kienle§

University of Siegen, Inorganic Chemistry I, Adolf-Reichwein-Strasse 2, 57068 Siegen, Germany, and Max-Planck-Institute for Solid State Research, Heisenbergstrasse 1, 70569 Stuttgart, Germany

Received June 6, 2007

$PdBr_2Se_6$ and $PdCl_2Se_8$ are two new compounds with cyclic Se_6 coordinated to $PdBr_2$ molecules and one-dimensional helical Se_x chains coordinated to $PdCl_2$ molecules. $PdBr_2Se_6$ is a black solid with a crystal structure similar, but not equal, to $PdCl_2Se_6$. It crystallizes in the space group $P\bar{1}$ with the lattice constants $a = 4.3946(8)$ Å, $b = 7.605(1)$ Å, $c = 7.992(2)$ Å, $\alpha = 66.15(2)°$, $\beta = 86.44(2)°$, $\gamma = 80.90(2)°$, and $Z = 1$ and can be handled in air like the deep red $PdCl_2Se_8$ which crystallizes in the orthorhombic space group *Pbca* with the lattice constants $a = 9.609(2)$ Å, $b = 8.958(2)$ Å, $c = 13.799(3)$ Å, and $Z = 4$. In $PdBr_2Se_6$, two cyclic Se_6 molecules (chair conformation) are directly coordinated to Pd atoms, forming $Pd(Se_6)_2Br_2$ groups. These are connected to one-dimensional chains via trans-standing Se atoms. In $PdCl_2Se_8$, the selenium substructure consists of helical chains with every fifth Se atom directly coordinated to the Pd atom of a $PdCl_2$ group. Each $PdCl_2$ group on the other hand connects two neighboring Se_x helices. The type of Se_x helix found for this compound is unique and differs from all other ones reported up to now including elemental α-Se. A reproducible twinning observed for $PdBr_2Se_6$ crystals in the course of the X-ray single-crystal investigations is checked by transmission electron microscopy in connection with details of the atomic arrangement. The Raman spectra of $PdBr_2Se_6$ and $PdCl_2Se_8$ are compared to Raman data of elemental Se modifications and give significant support for the Se_6 and helical Se_x to be neutral molecules. A discussion of the results of thermal analyses gives clear evidence that cyclic Se_6 and helical Se_x are considerably stabilized by bonding to the PdX_2 molecules because the melting temperatures of the composite materials are significantly higher than the ones of the respective elemental modifications.

Introduction

In the course of earlier research work to improve the ionic conductivity of Cu(I) halides and chalcogenides, a class of crystalline compounds was discovered that can structurally be rationalized as composite materials with two clearly separated partial structures on a nanometer scale. One partial structure consists of neutral molecules of group 16 elements, the other one of a neutral Cu(I) halide (e.g., $CuClSe_2$ with a CuCl partial structure and infinite helical molecules Se_x). Such compounds were also termed as "adducts" or "nanocomposites" in which "neutral chalcogen molecules" are embedded in a "matrix of a Cu(I) halide" (Table 1).

A considerable variety of compounds with Cu(I) halides but only one with a Ag(I) halide was obtained in the past. With $(AgI)_2Se_6$ (=$AgISe_3$) and $(AgI)_2Te_6$ (=$AgITe_3$), we recently published two new examples containing Ag(I) halides.[1] Further research work demonstrated that $PdCl_2$ can also be a suitable partner for the inclusion of neutral chalcogen molecules (cyclic Se_6 in $PdCl_2Se_6$[2]). Many of the respective syntheses were carried out under *supercritical* hydrothermal conditions in acidic media at temperatures between 400 and 500 °C.

In this paper we present the structure and properties of two additional new compounds that were initially prepared in our group under *subcritical* hydrothermal conditions (~200 °C) in concentrated hydrogen halide acids. $PdBr_2Se_6$

† Dedicated to Prof. Rudolf Hoppe on the occasion of his 85th birthday.

* To whom correspondence should be addressed. E-mail: deiseroth@chemie.uni-siegen.de. Tel: +49-(0)271/740-4219. Fax: +49-(0)271/740-2555.

‡ University of Siegen.

§ Max-Planck-Institute for Solid State Research.

(1) Deiseroth, H. J.; Wagener, M.; Neumann, E. *Eur. J. Inorg. Chem.* **2004**, *24*, 4755−4758.

(2) Neininger, K.; Rotter, H. W.; Thiele, G. *Z. Anorg. Allg. Chem.* **1996**, *622*, 1814−1818.

10.1021/ic701108c CCC: $37.00
Published on Web 08/17/2007

Table 1. Summary of Known Nanocomposites with Neutral Se_x and Te_x Molecules

compound	neutral Ch unit	ref
CuClTe	Te_x helix	4
CuBrTe	Te_x helix	5
CuITe	Te_x helix	6,7
$CuClSe_2$	Se_x helix	8
$CuBrSe_2$	Se_x helix	9
$CuClTe_2$	Te_x helix	10
$CuBrTe_2$	Te_x helix	11
$CuITe_2$	Te_x helix	11
$CuBrSe_3$	cyclic Se_6	12,13
$CuISe_3$	cyclic Se_6	14
AgITe	Te_x helix	15
$AgISe_3$	cyclic Se_6	1
$AgITe_3$	cyclic Te_6	1
$PdCl_2Se_6$	cyclic Se_6	2
$PdBr_2Se_6$	cyclic Se_6	this work
$PdCl_2Se_8$	Te_x helix	this work
$Rb_3AsSe_4(Se_6)_2$	cyclic Se_6	16
$(Re_6Te_8)(TeCl_3)2Te_6$	cyclic Te_6	17
$K_3PSe_4(Se_6)_2$	cyclic Se_6	18
Cs_4Se_{16}	cyclic Se_6	19
Cs_3Te_{22}	cyclic Te_8	20
Cs_4Te_{28}	cyclic Te_8	21
$[Na(12\text{-crown-}4)^+]_2Se_8^{2-}\cdot(Se_6,Se_7)$	cyclic Se_6 and Se_7	22
$(NEt_4^+)_2[Se_5]^{2-}\cdot 1/2Se_6\cdot Se_7$	cyclic Se_6 and Se_7	23
$[Re_2I_2(CO)_6(Se_7)]$	cyclic Se_7	24
$[Ag_2(Se_6)(SO_2)_2][Sb(OTeF_5)_6]_2$	cyclic Se_6	25
$[Ag_2(Se_6)][AsF_6]_2$	cyclic Se_6	25
$[AgSe_6][Ag_2(SbF_6)_3]$	cyclic Se_6	25

contains cyclic Se_6 molecules and is structurally closely related to the already known $PdCl_2Se_6$. In $PdCl_2Se_8$, a new type of a one-dimensional infinite Se_x helix, different from all known elemental Se modifications, is found. Surprisingly, both new compounds can also be obtained by classical solid-state reactions starting from PdX_2 and elemental Se at moderate temperatures.

General Aspects

Besides the solids of the type mentioned in the introduction, a growing group of compounds was synthesized in which phosphorus-containing molecules[3] are stabilized in suitable matrices. The latter are not referenced in this paper. In Table 1, a summary of composite materials with neutral chalcogen molecules characterized by single-crystal investigations is presented. A close inspection of this table shows that the majority of compounds contains either helix-shaped polymeric Se_x/Te_x or cyclic Se_6 (all three known also as molecules in elemental modifications). Those with cyclic Se_6 form two groups. In one group, the Se_6 are directly coordinated to a Cu(I), Ag(I), or Pd(II); in the other group, the Se_6 behave more like "solvent molecules" with weak interactions to neighboring atoms. $K_3PSe_4(Se_6)_2$ with each Se atom of the cyclic Se_6 coordinated to a Se^{2-} of an adjacent $(PSe_4)^{3-}$ groups ($d > 3.20$ Å) is a typical example.

The cluster compound $(Re_6Te_8)(TeCl_3)_2Te_6$ is of particular interest because it was the first example with cyclic Te_6 molecules. $(AgI)_2Te_6$, as recently published by us, is the second example and, together with $(AgI)_2Se_6$, is only the third example containing a Ag(I) halide.[1] Cyclic Te_6 (chair conformation) including the crown-shaped Te_8 are *unknown* molecules in elemental Te modifications. In all these molecules, the bonding distances between chalcogen atoms are close to d(Se−Se) and d(Te−Te) in elemental modifications.

Working under *subcritical* hydrothermal conditions seems to be of great importance with respect to the existence of the just-mentioned Ag compounds and the title compounds of this paper. Interestingly, an earlier paper[26] reporting on compounds of the type CuI_xSe_y and based on syntheses under *supercritical* conditions stated "Similar compounds with Ag(I)-halides do not seem to exist". This statement is now disproved!

Problems concerning the nature of the (weak) chemical bonding interactions between the Se_6/Te_6 and the Cu(I)/Ag(I)/Pd(II) still wait for solution. A small but significant electron transfer from the chalcogen to the Cu/Ag atoms is very likely[27] and may be in particular important for the enhanced thermal stability of cyclic Se_6 as constituents in such solids (see below). For a small selection of Cu compounds (CuXSe, $CuXSe_2$, and $CuXSe_3$) the question of thermodynamical stability was treated on the basis of Se vapor pressure measurements[28] and thermal investigations of the respective phase diagrams. It turned out that the values of the standard enthalpies of formation referring to the components CuX and Se_x are small but negative (<50 kJ mol^{-1}). These values indicate a weak chemical bonding between the chalcogen molecules and Cu^+. If one concen-

(3) Pfitzner, A.; Bräu, M. F.; Zweck, J.; Brunklaus, G.; Eckert, H. *Angew. Chem., Int. Ed.* **2004**, *43*, 4228−4231.
(4) Milius, W. *Z. Anorg. Allg. Chem.* **1990**, *586*, 175−184.
(5) Carkner, P. M.; Haendler, H. M. *J. Solid State Chem.* **1976**, *18*, 183−189.
(6) Fenner, J.; Rabenau, A. *Z. Anorg. Allg. Chem.* **1976**, *426*, 7−14.
(7) Fenner, J.; Schulz, H. *Acta Crystallogr.* **1979**, *B35*, 307−311.
(8) Milius, W.; Rabenau, A. *Z. Naturforsch.* **1988**, *B43*, 243−244.
(9) Pfitzner, A.; Nilges, T.; Deiseroth, H. J. *Z. Anorg. Allg. Chem.* **1999**, *625*, 201−206.
(10) Fenner, J. *Acta Crystallogr.* **1976**, *B32*, 3084−3086.
(11) Milius, W. *Z. Naturforsch.* **1989**, *B44*, 990−992.
(12) Haendler, H. M.; Carkner, P. M. *J. Solid State Chem.* **1979**, *29*, 35−39.
(13) Sakuma, T.; Kaneko, T.; Kurita, T.; Takahashi, H. *J. Phys. Soc. Jpn.* **1991**, *60*, 1608−1611.
(14) Milius, W.; Rabenau, A. *Mater. Res. Bull.* **1987**, *22*, 1493−1497.
(15) Schnieders, F.; Böttcher, P. *Z. Kristallogr.* **1995**, *210*, 323−327.
(16) Wachhold, M.; Sheldrick, W. S. *Z. Naturforsch.* **1997**, *B52*, 169−175.
(17) Mironov, Y. V.; Pell, M. A.; Ibers, J. A. *Angew. Chem., Int. Ed. Engl.* **1996**, *35*, 2854−2856.
(18) Dickerson, C. A.; Fisher, M. J.; Sykora, R. E.; Albrecht-Schmitt, T. E.; Cody, J. A. *Inorg. Chem.* **2002**, *41*, 640−642.
(19) Sheldrick, W. S.; Braunbeck, H. G. *Z. Naturforsch.* **1989**, *B44*, 1397−1401.
(20) Sheldrick, W. S.; Wachhold, M. *Angew. Chem., Int. Ed. Engl.* **1995**, *34*, 450−451.
(21) Sheldrick, W. S.; Wachhold, M. *Chem. Commun.* **1996**, *5*, 607−608.
(22) Staffel, R.; Müller, U.; Ahle, A.; Dehnicke, K. *Z. Naturforsch.* **1991**, *B46*, 1287−1292.
(23) Dietz, J.; Müller, U.; Müller, V.; Dehnicke, K. *Z. Naturforsch.* **1991**, *B46*, 1293−1299.
(24) Bacchi, A.; Baratta, W.; Calderazzo, F.; Marchetti, F.; Pelizzi, G. *Angew. Chem., Int. Ed. Engl.* **1994**, *33*, 193−195.
(25) Aris, D.; Beck, J.; Decken, A.; Dionne, I.; Krossing, I.; Passmore, J.; Rivard, E.; Steden, F.; Wang, X. *Phosphorus, Sulfur Silicon Relat. Elem.* **2004**, *179*, 859−863.
(26) Rabenau, A.; Rau, H.; Kershaw, R.; Wold, A. *Inorg. Synth.* **1973**, *14*, 160−173.
(27) Wagener, M. Ph.D. thesis, University of Siegen, Siegen, Germany, 2005.
(28) Rabenau, A.; Rau, H.; Rosenstein, G. *Z. Anorg. Allg. Chem.* **1970**, *374*, 43−53.

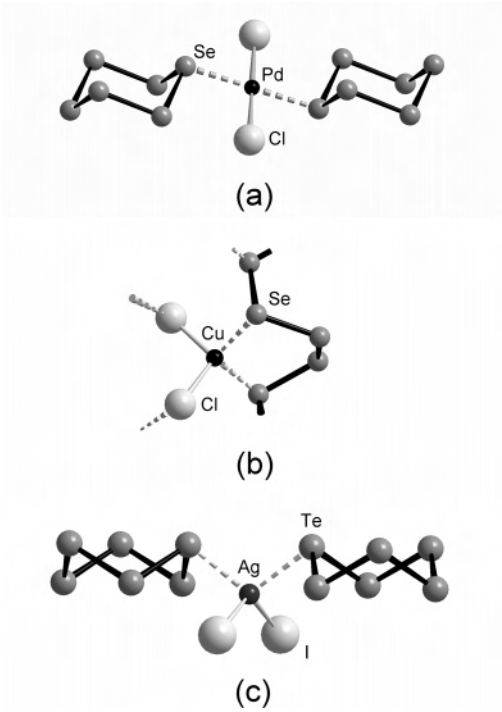

Figure 1. Examples for the local coordination around Pd^{2+} in $PdCl_2Se_6$ (a), Cu^+ in $CuClSe_2$ (b), and Ag^+ in $AgITe_3$ (c).

trates on the local coordination around the d^8 or d^{10} ions, it turns out that the respective chalcogen molecules act like neutral ligands (NH_3, CO, etc.) in classical coordination compounds. They just complete the coordination sphere of the central atom (Figure 1). However, monomeric molecules of the type shown in Figure 1a and c are unknown; instead they tend to form one-, two-, or three-dimensional polymers (see below).

A further open problem with such solids concerns the question which compounds might be suitable as bonding partners for the neutral elemental molecules beside the ones which have been found more or less by accident in the past. The examples cited in Table 1 are indications that the Pearson concept of hard and soft Lewis acids and bases[29] might be a suitable basis for an understanding of the experimental results and further planning of syntheses. In the frame of this model, d^8 and d^{10} cations, as well as Cs^+, $[Re_6]^{2+}$, and $[NR_4]^+$ are *soft Lewis acids* reacting preferably with the *soft Lewis bases* Se_6, Te_6, etc.

Until now it was not possible to separate one of the Se_x or Te_x molecules from its metal halide component without decomposition of the whole compound. This would be particularly important in the case of cyclic Te_6, which does not exist in one of the known elemental modifications. Interestingly the extraction of a new phosphorus modification from a CuI matrix was recently reported to be successful.[3]

Experimental Section

Sample Preparation. $PdBr_2Se_6$ and $PdCl_2Se_8$ can be prepared as main constituents of heterogeneous mixtures by hydrothermal syntheses in concentrated hydrogen halide acid. For reference purposes (Raman, DTA), the already-known $PdCl_2Se_6$ was also prepared. Surprisingly, the alternative preparation by classical solid-state reactions (without any solvent) was also possible and resulted in products with significant lower contamination by other phases.

The hydrothermal syntheses of both title compounds were carried out in quartz glass ampoules, by heating stoichiometric mixtures of about 0.5 g of overall product, using Pd (99%, CHEMPUR) [0.023 g for $PdBr_2Se_6$ and 0.018 g for $PdCl_2Se_8$], Se (99% MERCK) [0.187 g for $PdBr_2Se_6$ and 0.200 g for $PdCl_2Se_8$], and SeO_2 (98% MERCK) [0.024 g for $PdBr_2Se_6$ and 0.019 g for $PdCl_2Se_8$], together with an excess of the respective concentrated hydrogen halide acid (~0.3 mL) [HBr (48% ACROS) or HCl (37% RIEDEL DE HAEN)]. Subsequently, the sealed ampoules were transferred to a steel autoclave and then kept at 453 K for 5 days. The crystals obtained for $PdBr_2Se_6$ were black, rectangular-shaped, and air-stable. For $PdCl_2Se_8$, a variety of air-stable, deep red-violet crystals with various well-defined shapes were obtained. Selected crystals from the hydrothermal preparations were used for X-ray single-crystal investigations and structure refinements.

The solid-state syntheses of both title compounds were carried out by forming compact pellets with stoichiometric amounts for 0.8 g of overall product by using PdX_2 (X = Br or Cl) [For $PdBr_2Se_6$, 0.288 g of $PdBr_2$ (39.8−40.1% Pd, ACROS) and for $PdCl_2Se_8$, 0.175 g of $PdCl_2$ (59.83% Pd, CHEMPUR)], and Se (99.9% Fluka) [0.512 g for $PdBr_2Se_6$ and 0.625 g for $PdCl_2Se_8$]. The pellets were heated in sealed quartz glass ampoules in a tube oven at 423 K for 10 days. The products were microcrystalline and nearly, but not completely, phase pure in standard X-ray powder diagrams. In contrast to the products from hydrothermal syntheses, the crystals were, however, too small to perform an X-ray single-crystal determination.

Single-Crystal X-ray Investigations. Crystals of both compounds ($PdCl_2Se_8$ and $PdBr_2Se_6$) were measured with a STOE IPDS diffractometer using graphite-monochromated Mo Kα radiation (λ = 0.71073 Å). The STOE IPDS program package[30] was used to analyze the measured data. A close examination of reciprocal space by using the program RECIPE[30] did not show any anomalies in the case of $PdCl_2Se_8$. A routine structure solution and refinement using SHELX97[31] resulted in the described structure model. A summary of crystal and structure refinement data for $PdCl_2Se_8$ is reported in Tables 2 and 3.

In contrast to $PdCl_2Se_8$, all examined crystals of $PdBr_2Se_6$ (five crystals were measured) were twinned and showed overlapping and interpenetrating reflections in the reciprocal space. In all cases, a similar systematic twinning with an approximate volume ratio of the twinned domains of 1:1 could be observed. The programs INDEX and CELL[30] were used to index the lattices and to obtain the orientation matrices for the twin components. The superposition of the reciprocal lattices is shown in Figure 2.

All reflections with *hkl*, $h = 7n$ coincide within the measuring accuracy exactly, while the remaining reflections are well separated or partly overlapped, respectively. An analysis of the reciprocal space with the program ROTAX[32] to test for possible twin laws comes to the result that the description of the observed twinning with the twin law (−1 0 0)(0 −1 0)(0.003 −0.855 1) is the most

(29) Pearson, R. G. *Survey Progr. Chem.* **1969**, *5*, 1−52.

(30) *IPDS Software*, Version 2.93; STOE and Cie: Darmstadt, Germany, 1999.
(31) Sheldrick, G. M. *SHELX-97, Program Package for the Solution and Refinement of Crystal Structures*; University of Göttingen: Göttingen, Germany, 1997.
(32) Cooper, R. I.; Gould, R. O.; Parsons, S.; Watkin, D. J. *J. Appl. Crystallogr.* **2002**, *35*, 168−174.
(33) *X-RED 1.19*; STOE and Cie: Darmstadt, Germany, 1999.
(34) *X-SHAPE 1.06*; STOE and Cie: Darmstadt, Germany, 1999.

Table 2. Crystallographic Data and Details of the Structure Determination for $PdCl_2Se_8$ and $PdBr_2Se_6$

	$PdCl_2Se_8$	$PdBr_2Se_6$
fw	808.98 g/mol	739.98 g/mol
color	deep red	black
Pearson code	*o*P44	*a*P9
cryst syst	orthorhombic	triclinic
space group	*Pbca* (No. 61)	$P\bar{1}$ (No. 2)
unit cell dimens	$a = 9.609(2)$ Å	$a = 4.3946(8)$ Å
	$b = 8.958(2)$ Å	$b = 7.605(1)$ Å
	$c = 13.799(3)$ Å	$c = 7.992(2)$ Å
		$\alpha = 66.15(2)°$
		$\beta = 86.44(2)°$
		$\gamma = 80.90(2)°$
V	1187.8(4) Å^3	241.21(8) Å^3
Z	4	1
ρ_{calcd}	4.524 g/cm^3	5.094 g/cm^3
diffractometer	IPDS (STOE)	
λ	0.71073 (Mo Kα)	
monochromator	graphite	
cryst size	0.23 × 0.12 × 0.09 mm^3	0.10 × 0.03 × 0.02 mm^3
measuring temp	$T = 296(2)$ K	
scan type	φ-scan	
measured θ-range	$2.95° \le \theta \le 30.39°$	$2.96° \le \theta \le 30.34°$
index ranges	$-13 \le h \le 12$	$-6 \le h \le 6$
	$-10 \le k \le 12$	$-10 \le k \le 10$
	$-19 \le l \le 19$	$-11 \le l \le 11$
reflns collected	9535	2412
independent reflns	1777	977
observed reflns	1245 [$I > 2\sigma(I)$]	556 [$I > 2\sigma(I)$]
data averaging[a]	$R_{int} = 0.0835$	$R_{int} = 0.1007$
	$R_\sigma = 0.0545$	$R_\sigma = 0.1305$
completeness to θ_{max}	99.1%	67.1%
abs coeff	$\mu = 26.468$ mm^{-1}	$\mu = 32.759$ mm^{-1}
abs correction	numerical[33,34]	
transmission factors	$0.0242 \le T \le 0.1649$	$0.2179 \le T \le 0.6021$
extinction coeff	$\epsilon = 0.0005(2)$	$\epsilon = 0.005(1)$
structure solution	direct methods[31]	
structure refinement	full-matrix least-squares on F^2 [31]	
no. of params	53	44
no. of restraints	0	0
GOF on F^2	0.916	0.858
$F(000)$	1408	320
weighting Scheme[b]	$A = 0.0471$, $B = 0$	$A = 0.0561$, $B = 0$
fig. of merit[a] [$I > 2\sigma(I)$]	$R_1 = 0.0360$, $wR_2 = 0.0766$	$R_1 = 0.0496$, $wR_2 = 0.1045$
fig. of merit[a] [all data]	$R_1 = 0.0635$, $wR_2 = 0.0846$	$R_1 = 0.1023$, $wR_2 = 0.1193$
residual electron density	$-1.359 \le \rho \le 1.614$ e/Å^3	$-2.188 \le \rho \le 1.430$ e/Å^3

[a] For the definition of R factors, see ref 31. [b] $w = 1/[\sigma^2(F_0^2) + (AP)^2 + BP)]$, $P = (F_0^2 + 2F_c^2)/3$.

Table 3. Wyckoff Positions (WP), Coordinates, and Equivalent Displacement Parameters U_{eq} (Å^2) for $PdCl_2Se_8$ (sof = 1; for the final Refinement all Occupation Factors which are one within the Threefold Deviation, are fixed)

atom	WP	*x*	*y*	*z*	U_{eq}[a]
Pd(1)	4*b*	0	0	0.5	0.0192(2)
Se(1)	8*c*	0.01911(7)	0.20346(7)	0.61619(5)	0.0208(2)
Se(2)	8*c*	0.15569(8)	0.37717(7)	0.52947(5)	0.0218(2)
Se(3)	8*c*	0.11936(7)	0.58807(7)	0.62665(5)	0.0227(2)
Se(4)	8*c*	0.18578(8)	0.08927(9)	0.72526(5)	0.0273(2)
Cl(1)	8*c*	0.1552(2)	0.1014(2)	0.3909(1)	0.0325(4)

[a] U_{eq} is defined as one-third of the trace of the orthogonalized U_{ij} tensor: $U_{eq} = {}^1/_3\Sigma_i\Sigma_j U_{ij} a_i^* a_j^* \mathbf{a}_i \mathbf{a}_j$.

probable. This twin law corresponds to a 180° rotation along [001]*. A structure solution[31] on the basis of an (for twinning) uncorrected dataset resulted in a suitable structure model. The observed systematic extinctions are consistent with the space groups *P*1 and $P\bar{1}$, of which the latter centrosymmetric one was chosen. This choice was supported by means of the distribution of the normalized structure factors. The following structure refinement[31] with the same data set converged, however, as already expected, with only unsatisfactory quality factors. Integration of all data on the basis of a specific domain matrix without rejecting overlapping reflections by the program INTEGRATE[30] and a following refinement using the SHELX HKLF 5 format did not lead to a satisfying result because of the partially overlapping reflections. In the case of a non-merohedric twinning, the program TWIN[30] allows a simultaneous integration of reflections from all twin domains by rejecting all completely and partly overlapping ones. Using this strategy, the result of the refinement is satisfactory, although the dataset is incomplete. A summary of crystal and structure refinement data for one of the five measured $PdBr_2Se_6$ crystals is reported in Tables 2 and 4. Further details of the crystal structure investigations including anisotropic thermal parameters may be obtained from the Fachinformationszentrum Karlsruhe D-76344 Eggenstein-Leopoldshafen, Germany, on quoting the depository numbers CSD-418159 ($PdCl_2Se_8$) and CSD-418160 ($PdBr_2Se_6$).

Raman Spectroscopy. Raman vibrational spectroscopy for suitable crystalline samples was done on a Bruker Raman Fourier-transform spectrometer RFS 100/S. The samples were ground in agate mortars and subsequently filled in glass capillaries which were sealed from one end. The capillaries were later placed in the sample holder of the instrument, and the beam of Nd:YAG laser ($\lambda = 1064$ nm) was used as excitation source.

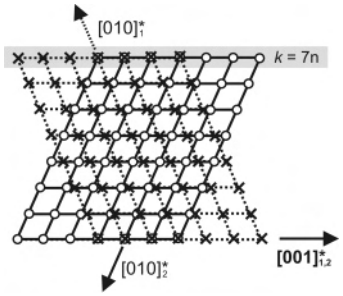

Figure 2. Superposition of the reciprocal lattices for the twinned domains (1, 2) of $PdBr_2Se_6$, projection along $[1\ 0\ 0]_1$* and $[-1\ 0\ 0]_2$*, respectively. All reflections with *hkl*, $h = 7n$ coincide within the measuring accuracy exactly.

Table 4. Wyckoff Positions (WP), Coordinates, and Equivalent Displacement Parameters U_{eq} (Å^2) for $PdBr_2Se_6$ (sof = 1; for the final Refinement all Occupation Factors which are one within the Threefold Deviation, are fixed)

atom	WP	*x*	*y*	*z*	U_{eq}[a]
Pd(1)	1*b*	0	0	0	0.0188(4)
Se(1)	2*i*	0.1715(4)	0.2176(2)	0.4862(2)	0.0235(4)
Se(2)	2*i*	0.9384(4)	0.4858(2)	0.2386(2)	0.0241(4)
Se(3)	2*i*	0.8420(4)	0.2701(2)	0.7151(2)	0.0201(4)
Br(1)	2*i*	0.5989(4)	0.1633(2)	0.1356(2)	0.0260(5)

[a] U_{eq} is defined as one-third of the trace of the orthogonalized U_{ij} tensor: $U_{eq} = {}^1/_3\Sigma_i\Sigma_j U_{ij} a_i^* a_j^* \boldsymbol{a}_i \boldsymbol{a}_j$.

Thermal Analysis (DTA). The measurements were done with a DTA L-62 (Linseis, Selb) device. The samples were sealed in small quartz glass ampoules ($d = 2$ mm, $l = 20$ mm) and measured in the temperature range from room temperature to 280 °C with a heating/cooling rate of 5 °C/min.

Transmission Electron Microscopy. A bulk sample was crushed and suspended in *n*-butanol for TEM preparation. HRTEM and SAED (selected area electron diffraction) were performed with a Philips CM 30ST microscope (300 kV, LaB_6 cathode, $C_S = 1.15$ mm). HRTEM micrographs were simulated with the EMS program package[35] (multislice formalism, spread of defocus, 70 Å; illumination semiangle, 1.2 mrad). All images were recorded with a Multiscan CCD camera and evaluated with the program Digital Micrograph 3.6.1 (Gatan). Elemental analyses by EDX were performed in the nanoprobe mode of CM 30ST with a Si/Li detector (Noran, Vantage System).

Results and Discussion

Crystal Structure of $PdBr_2Se_6$. $PdBr_2Se_6$ crystallizes in the triclinic space group $P\bar{1}$. The crystal structure of $PdBr_2Se_6$ is closely related to the known structure of $PdCl_2Se_6$, although the space group for the latter one is $P2_1/c$. In both compounds, the Pd atom is located at a center of inversion. The local coordination around Pd is similar for both compounds (Figure 3) and characterized by a distorted square planar coordination of two Se (from two separate Se_6) and two Br atoms. The only difference concerns the increase of the distances *d*(Pd−Cl) from 2.29 Å to *d*(Pd−Br) = 2.45 Å whereas the *d*(Pd−Se) and *d*(Se−Se) and comparable bond angles are nearly the same (Table 5). Within the Se_6 rings, three different Se−Se distances are observed for both structures. The distances between the uncoordinated Se atoms, *d*(Se1−Se2) = 2.33 Å, are significantly shorter than the distances *d*(Se(3)−Se(2)) and *d*(Se(3)−Se(1)) (around 2.38 Å).

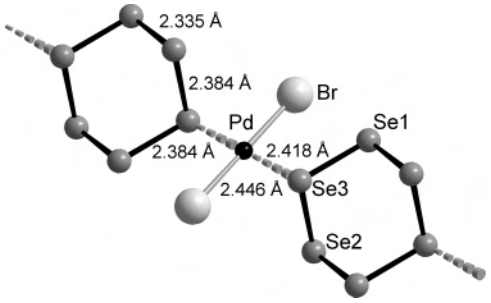

Figure 3. Local coordination around Pd in $PdBr_2Se_6$.

Table 5. Important Interatomic Distances (Å) and Angles (deg) for $PdBr_2Se_6$ and $PdCl_2Se_6$[2] [a]

	$PdBr_2Se_6$	$PdCl_2Se_6$
Distances (Å)		
Pd(1)−*Hal*(1)	2.446(1)	2.292(9)
−Se(3)	2.419(2)	2.421(4)
Se(3)−Se(2)	2.383(2)	2.381(5)
Se(2)−Se(1)	2.335(2)	2.327(6)
Se(1)−Se(3)	2.383(2)	2.377(5)
Angles (deg)		
Hal−Pd−Se(3)	95.42(6)	94.3(3)
Hal−Pd−Se(3)	84.58(6)	85.7(3)
Pd(1)−Se(3)−Se(2)	98.54(7)	97.6(2)
Pd(1)−Se(3)−Se(1)	105.86(6)	102.7(2)
Se(3)−Se(2)−Se(1)	97.76(9)	98.8(2)
Se(2)−Se(1)−Se(3)	96.22(7)	97.7(2)
Se(1)−Se(3)−Se(2)	101.84(9)	101.4(2)

[a] Both compounds do not crystallize isotypically but show comparable ${}^1_\infty[Pd(Se_6)_{2/2}X_2]$ chains.

The monomers are connected to one-dimensional infinite chains ${}^1_\infty[Pd(Se_6)_{2/2}X_2]$ via opposite Se atoms of the respective cyclic Se_6. These chains are oriented parallel to [0 1 0] in $PdCl_2Se_6$ and parallel to [0 −1 1] in $PdBr_2Se_6$. Their topology is clearly reminiscent of similar chains in the compound catena-poly[(Ag-μ-piperazine-κ^2-*N*,*N*′)perchlorate] where the cyclic Se_6 are replaced by piperazine groups.[36] An inspection of the three-dimensional packing of the chains (Figure 4) shows that the main difference between $PdCl_2Se_6$ and $PdBr_2Se_6$ concerns their spatial arrangement. In contrast to $PdCl_2Se_6$, adjacent chains in $PdBr_2Se_6$ show a similar orientation. In the former one, neighboring chains are transformed by a $2_1/c$ operation into each other. The different orientation can be easily visualized by comparing the projections of the two structures along [−1 0 0]. In this projection, the connecting lines Br−Pd−Br of $PdBr_2Se_6$ are orientated parallel to each other while the connecting lines Cl−Pd−Cl of neighboring ${}^1_\infty[Pd(Se_6)_{2/2}X_2]$ chains in $PdCl_2Se_6$ correspond to a zigzag pattern.

Transmission Electron Microscopy on $PdBr_2Se_6$. EDX analyses confirmed the nominal composition of the bulk sample. The average of six point measurements on six crystals gave Pd, 11.8(1.6) atom %; Br, 22.2(1.0) atom %;

(35) Stadelmann, P. A. *Ultramicroscopy* **1987**, *21*, 131.
(36) Liu, J. T.; Ng, S. W. *Acta Crystallogr.* **2006**, *E62*, 1992−1993.
(37) Miyamoto, Y. *Jpn. J. Appl. Phys.* **1980**, *19*, 1813−1819.
(38) Lucovsky, G.; Mooradian, A.; Taylor, W.; Wright, G. B.; Keezer, R. C. *Solid State Comm.* **1967**, *5*, 113−117.

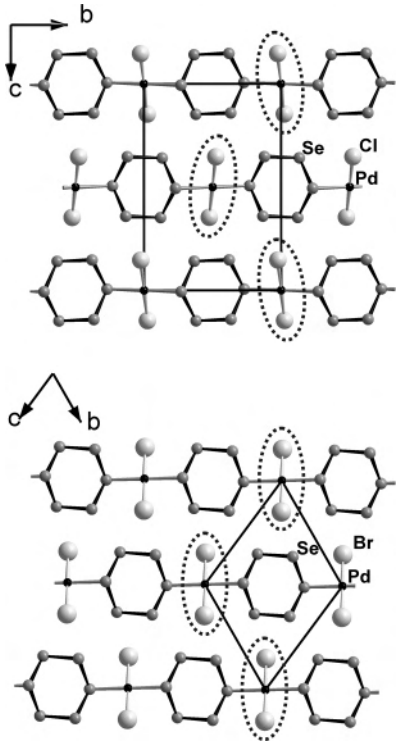

Figure 4. Comparison between $PdCl_2Se_6$ (upper) and $PdBr_2Se_6$ (lower) emphasizing the different tilts of the X−Pd−X lines (X = Cl, Br). In $PdCl_2Se_6$, the X−Pd−X fragments of neighboring $^1_\infty[Pd(Se_6)_{2/2}X_2]$ chains are alternately tilt to left and right; in $PdBr_2Se_6$ they are tilt parallel, see dashed ellipsoids.

and Se, 66.0(1.1) atom % (calculated values for the composition $PdBr_2Se_6$, 11.1; 22.2; 66.7 atom %). All SAED patterns contain Bragg intensities only and are consistent with the structure model derived from the X-ray study.

About 300 crystallites of $PdBr_2Se_6$ were tested for real structure phenomena, particularly for twinning (see above) and nanoscale intergrowth. Twin boundaries were never observed, even when scanning wide areas of the crystals in the medium-magnification mode. Hence, the systematic twinning found in the X-ray studies should rely on large domains which could break apart when grinding the sample for TEM preparation. HRTEM excludes the presence of "contaminating" domains with the related $PdCl_2Se_6$-type structure which could be easily identified if present (see Figure 5 for zone axes [100]). As exemplified for $PdBr_2Se_6$ in Figure 5a, the simulated contrasts (Figure 5a, left, $\Delta f = -40$ nm) approximate the projected potential map (Figure 5a, right). The bright spots correlate with the cavities in the centers of the Se_6 rings, see asterisks in Figure 5a, right, and their pattern can be used to distinguish the related structures. For the $PdBr_2Se_6$-type (Figure 5b, left), a characteristic deviation of 4.3° from the rectangular arrangement of the monoclinic $PdCl_2Se_6$ type (Figure 5b, right) is evident, which is also seen in the experimental micrograph of Figure 5c.

Crystal Structure of $PdCl_2Se_8$. Relevant X-ray data including atomic parameters, interatomic distances, and angles for the new solid $PdCl_2Se_8$ are summarized in Tables 2, 3, and 6. The orthorhombic crystal structure represents a new structure type.

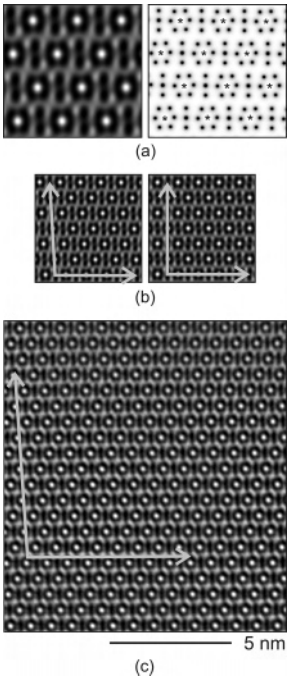

Figure 5. (a) Simulated micrograph and projected potential map for $PdBr_2Se_6$, (b) comparison of simulated micrographs based on the $PdBr_2Se_6$ and $PdCl_2Se_6$ types, and (c) experimental micrograph of $PdBr_2Se_6$. Parameters for simulations: [1 0 0] $\Delta f = -40$ nm, $t = 4.4$ nm. The arrows accent the different orientation of the chains in both compounds.

Table 6. Important Interatomic Distances (Å) and Angles (deg) for $PdCl_2Se_8$ (for Atom Types, See Figure 6)

	$PdCl_2Se_8$
Distances (Å)	
Pd(1)−Cl(6)	2.305(2)
Pd(1)−Se(1)	2.4343(8)
Se(1)−Se(2)	2.361(1)
Se(1)−Se(4)	2.424(1)
Se(2)−Se(3)	2.343(1)
Se(3)−Se(4)	2.315(1)
Angles (deg)	
Cl(1)−Pd(1)−Se(1)	85.05(5)
Cl(1)−Pd(1)−Se(1)	94.95(5)
Se(1)−Se(2)−Se(3)	99.12(4)
Pd(1)−Se(1)−Se(2)	101.63(3)
Pd(1)−Se(1)−Se(2)	98.21(3)
Se(2)−Se(3)−Se(4)	102.69(4)
Se(3)−Se(4)−Se(1)	99.87(4)
Se(4)−Se(1)−Se(2)	103.03(4)

As shown in Figure 6, the Se partial structure in this compound consists of one-dimensional infinite helical chains oriented parallel to the [0 1 0] direction of the orthorhombic unit cell. The chains are connected by Pd atoms in a way that layers perpendicular to [0 0 1] are formed. The shortest distances between neighboring layers are d(Se4−Cl) = 3.23 Å and d(Se3−Se4) = 3.57 Å. Every fourth Se atom of a Se chain is directly coordinated to a Pd atom and completes the coordination sphere of the Pd(II) together with a corresponding Se atom of a neighboring Se chain and two Cl atoms (d(Pd−Cl) = 2.31 Å, d(Pd−Se) = 2.43 Å). This situation results in a square planar coordination for each Pd(II) in accordance with $PdCl_2Se_6$ and $PdBr_2Se_6$ (Figure 7). The interatomic distances d(Se−Se) are in the range between 2.32 and 2.41 Å and thus are close to those

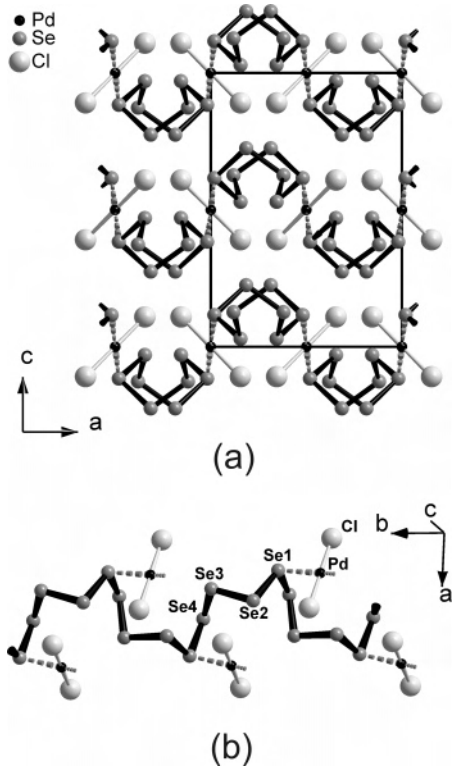

Figure 6. (a) Projection of the crystal structure of $PdCl_2Se_8$ along [0 1 0] emphasising the layered character of this compound. (b) Helical Se_x chain with connecting $PdCl_2$ groups emphasizing the attachment of Pd atoms to every fourth Se atom. Pd atoms drawn with only one Se partner connect to neighboring Se_x helices not shown in the figure.

ones in cyclic Se_6 molecules (2.33−2.39 Å), as well as in α-Se (2.37 Å).

It can be seen clearly from Figure 7 that the second coordination sphere of Pd (above and below the square plane) is completed by additional atoms from the Se_x chains. With d(Pd−Se) > 3.51 Å in comparison to d(Pd−Se) = 2.43 Å (first coordination sphere) they are not in a bonding distance.

If one compares the most relevant geometrical data of the new type of Se_x helix in $PdCl_2Se_8$ with those ones found in elemental α-Se and in $CuClSe_2$, one recognizes that the interatomic distances d(Se−Se) and thus the strengths of the covalent bonds Se−Se are more or less similar and vary between 2.32 and 2.42 Å ($PdCl_2Se_8$) and 2.32 and 2.39 Å ($CuClSe_2$) in comparison to 2.37 Å in helical α-Se and cyclic Se_6. However, the differences in conformation (in particular apparent from the torsion angles) point toward a considerable geometrical flexibility of the Se_x spiral. As a result of the different torsion angles, the density of Se atoms/Å along the chain axes is for $PdCl_2Se_8$ (0.89) and $CuClSe_2$ (0.86) significantly higher than for α-Se (0.61).

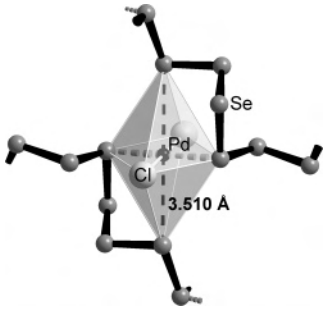

Figure 7. First and second coordination sphere of the Pd atoms in $PdCl_2Se_8$.

Raman Spectroscopy of $PdBr_2Se_6$ and $PdCl_2Se_8$. Table 7 gives a summary of Raman peaks including an earlier measurement of $PdBr_2Se_6$ (based on an unknown crystal structure at that time). As all relevant crystal structures have been solved in the meantime, we evaluate the Raman spectra primarily with respect to the question whether the cyclic Se_6 molecules in $PdBr_2Se_6$ and the one-dimensional infinite Se_x chains in $PdCl_2Se_8$ can be treated as matrix-stabilized variants of elemental molecules as the structures suggest. In this case, one would expect a certain matching between the wavenumbers of those vibrations that are mainly an indication for similar strengths of covalent Se−Se bond (similar d(Se−Se) see above) in these compounds and are not or only to a minor extend affected by symmetry influences inevitably present in the solid state.

The group of three peaks between 234 and 275 cm^{-1} (with minor differences between the referenced compounds) can most likely be assigned to ν_s(Se−Se) stretching vibrations in particular in comparison to trigonal Se (cyclic Se_6) and α-Se (Se_x helices). Apparently these peaks are *not* a fingerprint for the occurrence of cyclic Se_6 but more for the occurrence of covalent Se−Se bonds of similar strength. There is also good agreement for the ν_s(Pd−X) stretching vibrations and the ν_s(Pd−Se). Also the assignment of the deformation vibrations δ(Se−Se−Se) and δ(Se−Pd−X) between 102 and 144 cm^{-1} seems clear. There is, however, some ambiguity for the peak at 223 cm^{-1} appearing in the spectrum of $PdCl_2Se_8$, which contains four crystallographically independent Se atoms in contrast to only two in the other compounds.

Thermal Stability and Thermal Analyses. The elemental Se modification containing cyclic Se_6 molecules ("rhombohedral Se") is most likely not a thermodynamically stable one. According to earlier DTA (differential thermal analysis) investigations, it melts at 120 °C,[37] (endothermic). Further heating results in a recrystallization at about 135 °C

Table 7. Comparison of Raman Data (cm^{-1}) for Different PdX_2Se_x Compounds with Elemental Se

	$PdCl_2Se_6$[2]	$PdBr_2Se_6$[2]	$PdBr_2Se_6$	$PdCl_2Se_8$	$Se_{trigonal}$[37]	α-Se[38]
ν_s(Pd−X)	296	181	180	293		
ν_s(Pd−Se)	201	201	200	182		
ν(Se−Se)				223 (?)		
ν(Se−Se)	237	236	234	238	233	
ν(Se−Se)	256	251	249	245	237	239
ν(Se−Se)	275	275	272	266		254/249
δ(Se−Se−Se)	104	103	103	102		
δ(Se−Se−Se)	125	125	124	132		128
δ(X−Pd−Se)	144		143	141		

(exothermic) under formation of trigonal Se (helical chains), which melts finally at 217 °C. Our own DTA investigations of $PdBr_2Se_6$, $PdCl_2Se_6$, and $PdCl_2Se_8$ samples in sealed quartz glass ampoules give clear evidence that there is no significant thermal effect below 234 ($PdBr_2Se_6$), 243 ($PdCl_2Se_6$), and 248 °C ($PdCl_2Se_8$); hence, the incorporated cyclic Se_6 molecules and helical chains are stable up to this temperatures.

Upon further heating, the samples decompose irreversibly under formation of a heterogeneous product containing $PdSe_2$ among others as shown by powder X-ray investigations. This behavior is in general accordance to earlier TG (thermo gravimetry) experiments[2] using an Ar stream in an open system. These experiments proved a beginning decomposition at 200 °C and suggested tentatively the formation of $PdSe_2$. Summarizing the results, there is no doubt that cyclic Se_6 is stabilized by direct coordination to Pd^{2+} in composites like $PdBr_2Se_6$ and remains stable up to higher temperatures than in the elemental modification itself. Earlier thermal analyses with similar materials based on Cu(I) halides suggested even higher decomposition temperatures of 394 ($(CuI)_2Se_6$) and 338 °C ($(CuBr)_2Se_6$). Thus, it can be assumed that these solids are stable compounds in the quasi-binary tophase diagrams CuX−Se. As we surprisingly succeeded in preparing $PdCl_2Se_6$ and $PdBr_2Se_6$ not only under subcritical hydrothermal conditions but also by direct reaction between the respective Pd halide and α-Se (monoclinic, cyclic Se_8 molecules) at 150 °C (see Experimental Section), the existence of quasi-binary sections PdX_2−Se is most likely although not yet proven.

Acknowledgment. The authors are grateful to the "Deutsche Forschungsgemeinschaft" and the "Fonds der Chemischen Industrie" for their financial support.

IC701108C